Drug Design, Development and Therapy

Dovepress
Taylor & Francis Group

Open Access Full Text Article

ORIGINAL RESEARCH

# Formulation and Physicochemical Characterization of Capecitabine-Loaded Cubosomes for Enhanced Drug Delivery System

Ahmad Salawi

Department of Pharmaceutics, College of Pharmacy, Jazan University, Jazan, 45142, Saudi Arabia

Correspondence: Ahmad Salawi, Department of Pharmaceutics, College of Pharmacy, Jazan University, Jazan, 45142, Saudi Arabia, Email asalawi@jazanu.edu.sa



**Background:** Capecitabine (CPB) is a hydrophilic anticancer drug classified as Biopharmaceutics Classification System (BCS) Class III, which presents challenges for effective dermal delivery. Objectives: This study aimed to develop and characterize a topical cubosomal formulation encapsulating CPB to enhance its delivery efficiency. Significance: By evaluating in vitro release and permeation behavior, this work investigates the potential of CPB-loaded cubosomes as an innovative targeted drug delivery system capable of achieving higher localized drug concentrations.

**Methods:** CPB-loaded cubosomes were formulated using Pluronic F-68, Tween 80, and glyceryl monooleate. Four formulations were prepared by varying the concentrations of these excipients. A molten mixture of Pluronic F-68 and glyceryl monooleate was prepared, followed by incorporation of CPB under continuous stirring. The developed cubosomes were characterized for particle size, pH, zeta potential, viscosity, morphology (SEM), and in vitro drug release and permeation profiles.

**Results:** The optimized formulation exhibited a particle size of 177.66 nm, and SEM confirmed well-segregated, nanosized cubic structures. Drug release from the formulations ranged from 40% to 67%, while permeation efficiency varied from 50% to 92%, demonstrating enhanced dermal transport of CPB.

**Conclusion:** The CPB-loaded cubosomes demonstrated favorable physicochemical characteristics and significantly improved drug release and permeation, suggesting strong potential as an effective topical delivery system for capecitabine.

**Keywords:** capecitabine, cubosomes, pluronic F-68, cancer, drug release

## Introduction

Cancer remains the second leading cause of mortality in the United States, accounting for more than 600,000 deaths in 2022.[1–3] Among these, colorectal cancer (CRC) represents a significant burden, with approximately 50–60% of metastatic CRC (mCRC) patients progressing to advanced disease stages.[4–7] Antineoplastic drugs remain the foundation of cancer therapy, aiming to prolong survival and improve patient quality of life.[8–10] Capecitabine (CPB), an orally administered fluoropyrimidine carbamate and prodrug of 5-fluorouracil (5-FU), is widely used as a first-line monotherapy for advanced colorectal and colon cancers and in combination regimens for locally advanced or metastatic breast cancer.[11–14] After systemic absorption, CPB undergoes enzymatic conversion – primarily via thymidine phosphorylase, an enzyme overexpressed in many tumor tissues – resulting in intratumoral generation of 5-FU, thereby enhancing therapeutic selectivity and reducing systemic toxicity. The drug has a Tmax of approximately 1.5 hours and demonstrates less than 60% plasma protein binding, reflecting its concentration-dependent pharmacokinetics.[15,16] CPB is also used clinically in pancreatic cancer management and as a radiosensitizer in multimodal treatment strategies.[17–19] Its therapeutic efficacy depends on controlled activation into 5-FU, which inhibits DNA synthesis by targeting thymidylate synthase, ultimately suppressing tumor growth.[20–22]

Although CPB offers significant advantages over intravenous 5-FU, current delivery systems face several limitations, including inconsistent bioavailability, systemic adverse effects at higher doses, and limited ability to achieve sustained,

https://doi.org/10.2147/DDDT.S574417
Received: 15 October 2025
Accepted: 9 January 2026
Published: 21 January 2026

localized drug exposure. These challenges highlight the need for alternative drug-delivery platforms capable of improving the therapeutic index while reducing toxicity. Cubosomes have recently emerged as advanced lipid-based nanocarriers with promising applications in chemotherapy delivery, due to their high biocompatibility, structural versatility, ability to encapsulate both hydrophilic and lipophilic drugs, and potential for controlled and targeted release. Recent studies highlight their capacity to enhance dermal, transmucosal, and parenteral delivery of chemotherapeutics, making them attractive candidates for improving CPB delivery and reducing dose-dependent toxicity.

Cubosomes are self-assembled nanostructured particles formed by the hydration of glyceryl monooleate (GMO), which creates a three-dimensional bicontinuous cubic phase comprising intertwined lipid bilayers and two distinct aqueous channels.[23–25] This unique internal architecture allows tuning of drug release kinetics according to molecular weight and polarity.[26–28] Depending on composition and preparation, cubic phases can manifest as precursors, bulk gels, or dispersible nanoparticles (cubosomes).[29–31] Bulk cubic gels demonstrate excellent drug-loading capacity and stability due to their high viscosity, biodegradability, and ability to incorporate molecules of varying sizes.[32–35] However, their rigidity and limited spreadability restrict practical application, particularly for topical delivery.[36–39] Cubosomes, produced by dispersing cubic phases into aqueous media, preserve the internal nanostructure of the bulk gel while offering substantially improved fluidity, larger surface area, enhanced bioadhesion, and versatile administration routes including topical, parenteral, and intravenous delivery.[40–47] Despite these advantages, challenges such as controlling drug-release rates, stabilizing nanoparticle dispersions, and optimizing entrapment efficiency of hydrophilic drugs persist.[48–53] Considering these attributes and limitations, cubosomes represent a highly promising yet underexplored platform for the localized delivery of capecitabine. Enhancing dermal or transdermal delivery of CPB may improve drug targeting, reduce systemic burden, and allow higher local drug concentrations while mitigating adverse effects associated with oral dosing. This study aims to prepare and characterize CPB-loaded cubosomal formulations and to evaluate their physicochemical properties, in vitro drug release, and permeation behavior. By comparing four formulations with varying excipient compositions, this work seeks to assess their suitability as a topical drug-delivery system designed to enhance CPB deposition and controlled release.

# Methods

## Cubosome Preparation

Capecitabine-loaded cubosomes were prepared by systematically evaluating different ratios of glyceryl monooleate (GMO), Pluronic F-68, and Tween-80 to determine the most stable nanosystem. The method was adapted from previously validated cubosome preparation techniques, with modifications to improve drug incorporation efficiency and structural homogeneity.[54] Accurately weighed quantities of GMO and Pluronic F-68 (as listed in Table 1) were placed in a glass beaker and heated in a thermostatically controlled water bath at 70 °C. This step ensured complete melting of GMO and uniform mixing with Pluronic F-68, forming the precursor cubic gel. Maintaining the mixture above the lipid transition temperature was essential to promote proper bilayer fluidity and cubic phase formation. Once fully molten, the lipid–surfactant mixture was added dropwise to pre-heated distilled water (70 °C) under vigorous vortex mixing. High-energy mixing facilitated the spontaneous emulsification of the cubic gel into colloidal nanostructures. After complete addition, the dispersion was allowed to cool gradually to 25 °C, enabling self-assembly of cubosomal nanoparticles through thermodynamically driven reorganization of the lipid bilayers. Capecitabine was incorporated into the still-warm precursor phase by adding it gradually under continuous stirring. The system was mixed until a completely homogeneous dispersion was obtained, ensuring uniform drug distribution. Formulations were stored undisturbed for 48 hours at ambient temperature to allow full stabilization of the cubosome structure (Figure 1).

**Table 1** Composition of Cubosmes Formulations

| Formulations | Formulation 1 (F1) | Formulation 2 (F2) | Formulation 3 (F3) | Formulation 4 (F4) |
|---|---|---|---|---|
| Pluronic F68 (g) | 0.1 | 0.2 | 0.3 | 0.4 |
| Glyceryl monooleate (mL) | 1 | 1.5 | 2 | 2.5 |

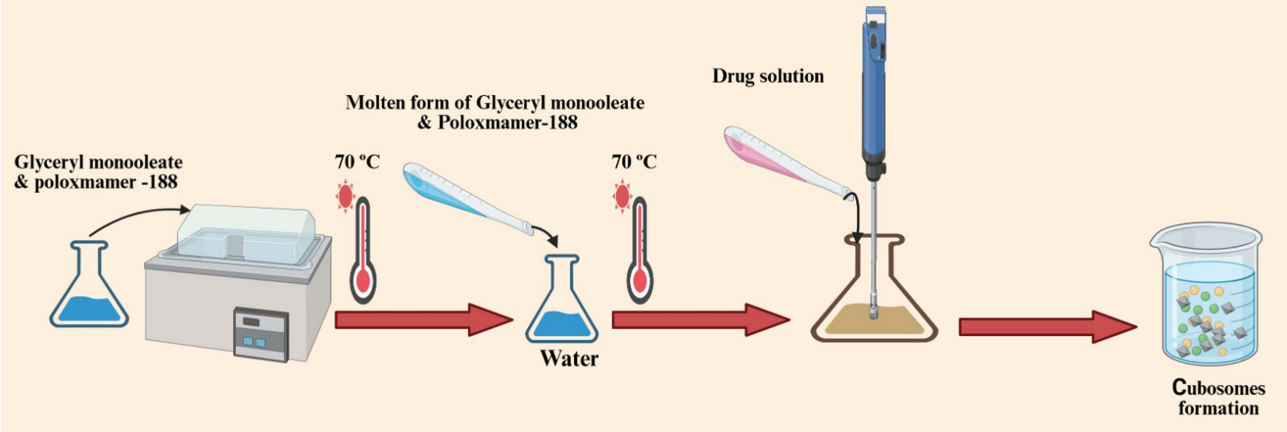


**Figure 1** Schematic representation of the stepwise preparation of cubosomes.

## Characterization of CPB/Pluronic F-68 Cubosomes

### pH Determination

The pH of each formulation was measured at 25 ± 0.5 °C using a calibrated pH meter. Physiological pH compatibility is crucial for topical formulations, as deviations can affect skin tolerance, drug permeation, and overall formulation stability.

### Viscosity Analysis

Viscosity measurements were performed at 25 ± 0.5 °C using a Brookfield Viscometer. The rheological behavior of cubosomal dispersions affects spreadability, drug release kinetics, and patient acceptability. Each sample was equilibrated before viscosity values were recorded in triplicate.

### Preparation of Capecitabine Calibration Curve

A calibration curve for capecitabine was prepared to enable accurate quantification during release and permeation studies. Stock solutions (1 mg/mL) were prepared in distilled water and serially diluted. Absorbance values were recorded at 266 nm using a UV–Vis spectrophotometer over the range of 200–400 nm. The resulting linear regression served as the reference for calculating drug content.

### Particle Size and Zeta Potential

Particle size distribution and zeta potential were determined by dynamic light scattering (DLS) using a Malvern Zetasizer Nano ZS. Samples were diluted 100-fold with distilled water to prevent multiple scattering. Measurements were performed at 25°C, and the mean hydrodynamic diameter and surface charge were calculated. DLS provides insight into colloidal stability, with zeta potential reflecting the degree of electrostatic repulsion that prevents particle aggregation.[54–56]

### Scanning Electron Microscopy (SEM)

SEM analysis was performed to examine the external morphology and surface characteristics of the cubosomes. A small drop of each formulation was placed on the SEM grid, dried at room temperature, and imaged under vacuum. This technique enabled visualization of nanosized cubic structures, confirming the formation of well-dispersed particles.

### X-Ray Diffraction (XRD)

XRD was used to investigate the crystalline behavior of capecitabine before and after formulation. Samples were scanned from 5° to 60° ($2\theta$) using Cu-Kα radiation. The loss of sharp crystalline peaks in the cubosomal formulation indicated successful drug encapsulation and partial amorphization, which is typically associated with improved solubility and dissolution behavior.[57]


https://doi.org/10.2147/DDDT.S574417

### Fourier Transform Infrared Spectroscopy (FTIR)

FTIR spectra were recorded to examine possible chemical interactions between CPB and excipients. Small quantities of each formulation were analyzed over 600–3800 $cm^{-1}$. Characteristic CPB peaks were evaluated for shifts or disappearance to confirm compatibility and the absence of chemical degradation.

## Stability Studies

### Centrifugation Test

Formulations were centrifuged at 5000 rpm for 30 minutes to assess physical stability. The absence of phase separation, sedimentation, or creaming indicated adequate structural integrity and emulsification efficiency.[58]

### Freeze–Thaw Stress

Cubosome dispersions were subjected to controlled stress cycling at –20 °C for 17 ± 2 hours, followed by heating at 40 °C for 1 hour. This procedure evaluates robustness against temperature-induced destabilization, such as coalescence or breakdown of the cubic nanostructure.[58–60]

### Differential Scanning Calorimetry (DSC)

DSC thermograms were obtained to evaluate thermal transitions, melting behavior, and potential drug–excipient interactions. Samples were heated from 25 to 400 °C at 10 °C/min under a nitrogen atmosphere. The disappearance of the sharp CPB melting peak confirmed embedding within the lipid matrix.[61]

## In vitro Drug Release

Drug release studies were conducted using a dialysis membrane technique. One milliliter of each formulation was placed inside a dialysis bag and immersed in 500 mL of distilled water maintained at 37 ± 0.5 °C on a USP dissolution apparatus (50 rpm). Samples were withdrawn at predefined intervals and analyzed at 266 nm to quantify cumulative release. Sink conditions were maintained by replacing the sampled volume with fresh medium.

## In vitro Permeation Studies

Permeation studies were performed using Franz diffusion cells. The donor compartment received 1 mL of formulation, while the receptor chamber contained PBS maintained at 37 °C. A hydrated cellophane membrane separated the compartments. Aliquots collected at specific intervals were analyzed by UV spectroscopy to quantify permeated drug, allowing calculation of flux and cumulative permeation.

# Results

## pH Analysis

The freshly prepared cubosomal formulations showed pH values ranging from 5.9 to 6.4 (Table 2), which are within acceptable dermal and mucosal tolerance limits. This mildly acidic pH indicates compatibility with skin physiology and reduces the risk of irritation or formulation-induced inflammatory responses during topical or transdermal application. The narrow pH range across formulations also suggests uniform composition and good stability of the dispersed cubosomal system.

**Table 2** pH and Viscosity Characteristics of the Prepared Formulations

| Formulations | pH value | Viscosity (cP) |
|---|---|---|
| F1 | 5.9 | 13.54 |
| F2 | 6.2 | 16.96 |
| F3 | 6.1 | 21.22 |
| F4 | 6.4 | 26.51 |

## Viscosity of Cubosomal Dispersions

The viscosities of the CPB-loaded cubosomes ranged from 13.54 to 26.51 cP (Table 2). Variations in viscosity correlated directly with the concentrations of Pluronic F-68 and glyceryl monooleate, indicating their structural contributions to the internal cubic matrix. Lower viscosity, as observed in F1 and F2, allows easier spreadability and rapid release of CPB from the lipid matrix, while the higher viscosity in F4 may enhance formulation retention at the application site and support sustained diffusion. These rheological properties collectively contribute to the functional performance of the cubosomal system.

## Linearity Curve of Capecitabine (CPB)

A calibration curve for CPB at 240 nm showed excellent linearity across the tested concentration range (Figure 2). The linear regression equation ($y = 0.0333x$) with an $R^2$ value of 1.0 confirms the reliability and high precision of the analytical method used to quantify CPB during release and permeation studies. This validated model ensured accurate determination of CPB concentrations in subsequent experiments.

## Zeta Potential and Particle Size Distribution

Dynamic light scattering analysis showed that the optimized CPB-loaded cubosomes had an average particle size of 177.66 nm, confirming their nanoscale dimensions suitable for enhanced permeation and cellular uptake (Figure 3B). The narrow distribution profile indicates good homogeneity of the formulation. The zeta potential distribution (Figure 3A), centered near neutrality, suggests that steric stabilization provided by Pluronic F-68 plays a dominant role in maintaining particle stability. Higher concentrations of Pluronic F-68 promoted the formation of smaller and more stable particles by improving interfacial stabilization during cubic-phase self-assembly.

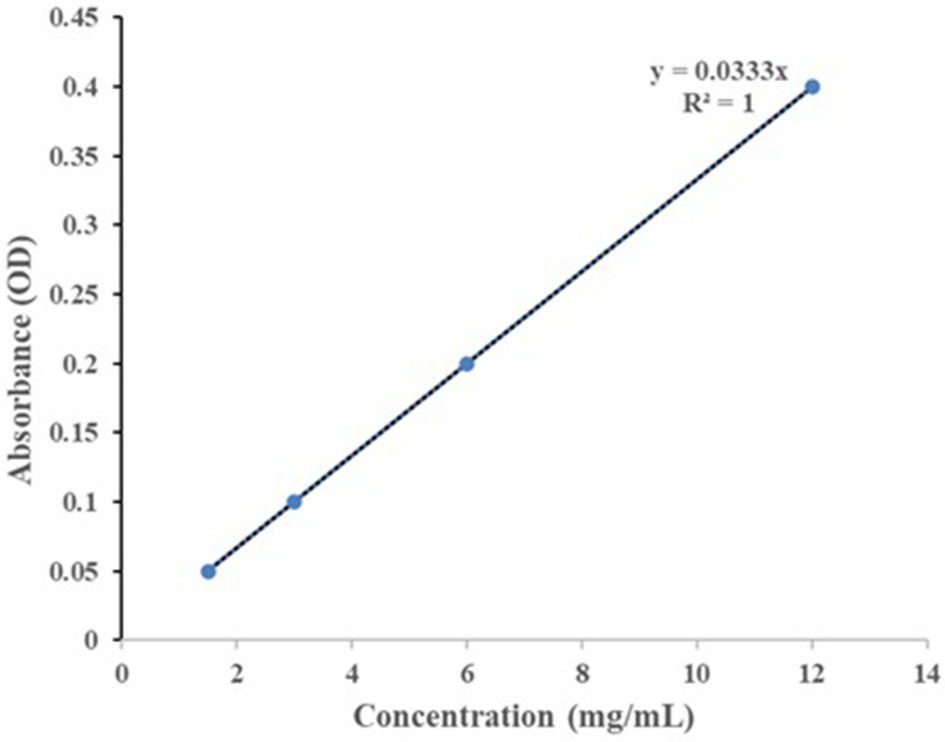


**Figure 2** Linearity curve of CPB.


https://doi.org/10.2147/DDDT.S574417

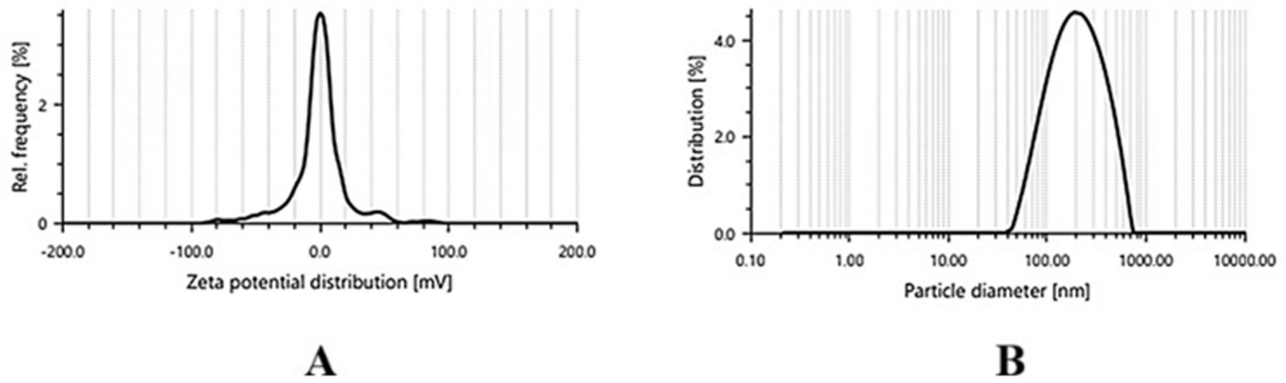


**Figure 3** (**A**) Zeta potential analysis of CPB-loaded cubosomes (**B**) Particle size distribution of CPB-loaded cubosomes.

## Scanning Electron Microscopy (SEM)

SEM micrographs (Figure 4) revealed well-defined nanoscale particles with characteristic cubic or cuboidal geometry, indicative of a successfully formed cubosomal system. The particles were highly uniform in shape, with clearly defined edges and smooth surface contours, reflecting a well-organized internal lipid arrangement during self-assembly. Several particles showed subtle surface texturing, suggesting the presence of bicontinuous internal channels, a hallmark of cubic-phase nanostructures. The particles were discrete and non-aggregated, confirming effective steric stabilization by Pluronic F-68 and glyceryl monooleate. The absence of collapsed, fused, or irregularly shaped particles indicates strong structural integrity and mechanical stability. Overall, the SEM images confirm that the formulation produced robust, monodisperse, cubic nanostructures with smooth, non-porous external morphology, demonstrating the successful creation of a stable cubosomal architecture capable of efficient drug encapsulation and delivery.

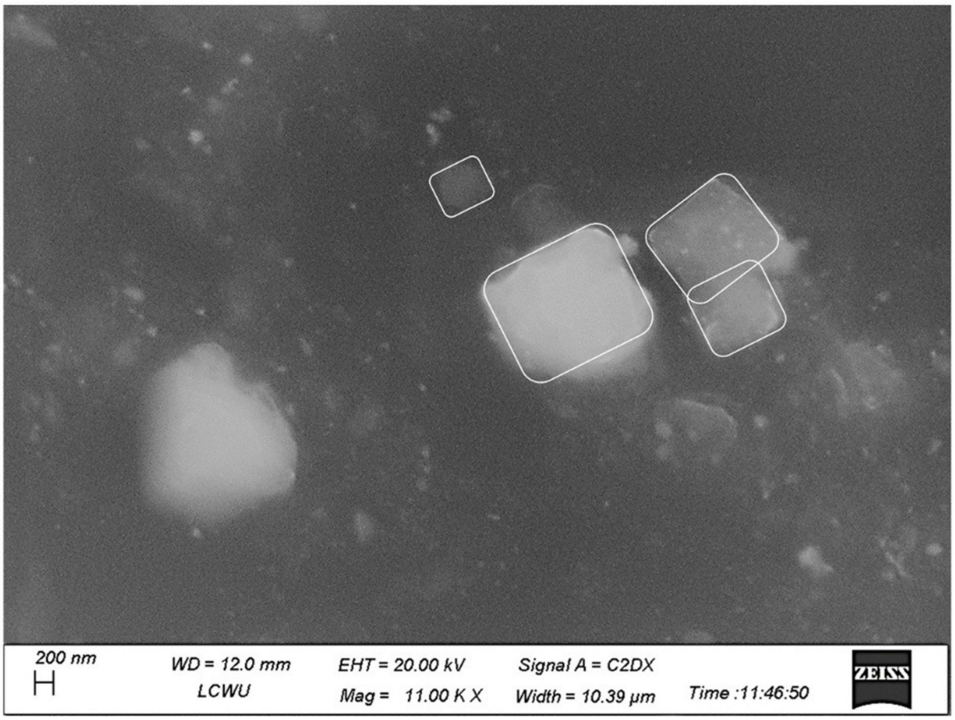


**Figure 4** Scanning electron microscopy (SEM) of CPB-loaded cubosomes.

## X-Ray Diffraction (XRD)

XRD analysis was performed to assess the crystalline behavior of CPB before and after incorporation into the cubosomal system (Figure 5). The diffractogram of pure CPB showed several sharp, well-defined peaks at 2$\theta$, 19.28°, 20.68°, 26.08°, and 28.3°, confirming its highly crystalline nature. These intense reflections are characteristic of an ordered lattice arrangement typically seen in unprocessed drug crystals. After encapsulation in the cubosomal matrix, the diffraction pattern changed significantly. The CPB-loaded cubosomes displayed a broad, diffuse scattering profile, with the prominent crystalline peaks completely disappearing. This altered pattern indicates an amorphous or molecularly dispersed drug state, suggesting that CPB was efficiently incorporated into the lipid bilayer and its crystalline structure was disrupted during formulation. The loss of crystallinity is a desirable outcome in nanocarrier systems, as the amorphous form of a drug generally has superior solubility, dissolution rate, and thermodynamic activity compared to its crystalline form. Additionally, the absence of residual crystalline domains reduces the risk of drug aggregation or recrystallization during storage, contributing to improved formulation stability. These findings confirm not only the successful encapsulation of CPB within the cubosomes but also a favorable physicochemical transition that supports enhanced drug performance and bioavailability.

## Fourier Transform Infrared Spectroscopy (FTIR)

FTIR spectra of the individual components (Tween 80, Poloxamer 188, glyceryl monooleate, and pure CPB) and the final cubosomal formulation are shown in Figure 6. Pure CPB exhibited characteristic peaks, including N–H stretching at 3523 $cm^{-1}$, O–H stretching at 3242 $cm^{-1}$, C–H stretching at 2926 $cm^{-1}$, and C=O stretching at 1775 $cm^{-1}$, along with C–O and C=C signature vibrations. Glyceryl monooleate showed its typical C=O peak at 1700 $cm^{-1}$ and a broad O–H band at 3320–3400 $cm^{-1}$, while Poloxamer showed aliphatic C–H and C–O stretching bands. The conserved peak positions in the cubosomal formulation, without significant chemical shifts or new peak formation, confirm the absence of incompatibility and lack of chemical interactions among CPB and excipients. This indicates that drug encapsulation occurs physically within the cubic structure rather than through chemical modification.

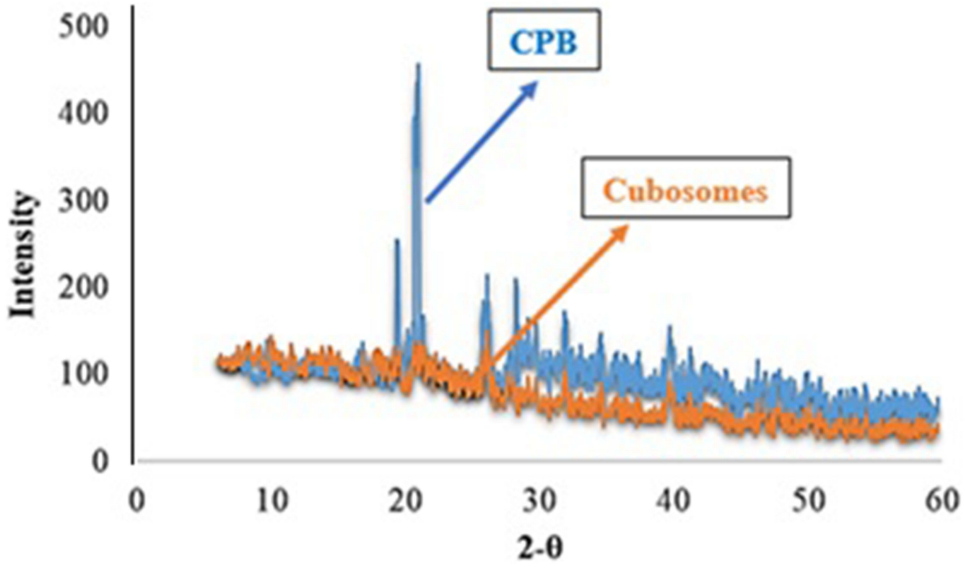


**Figure 5** X-ray diffraction (XRD) analysis.


https://doi.org/10.2147/DDDT.S574417

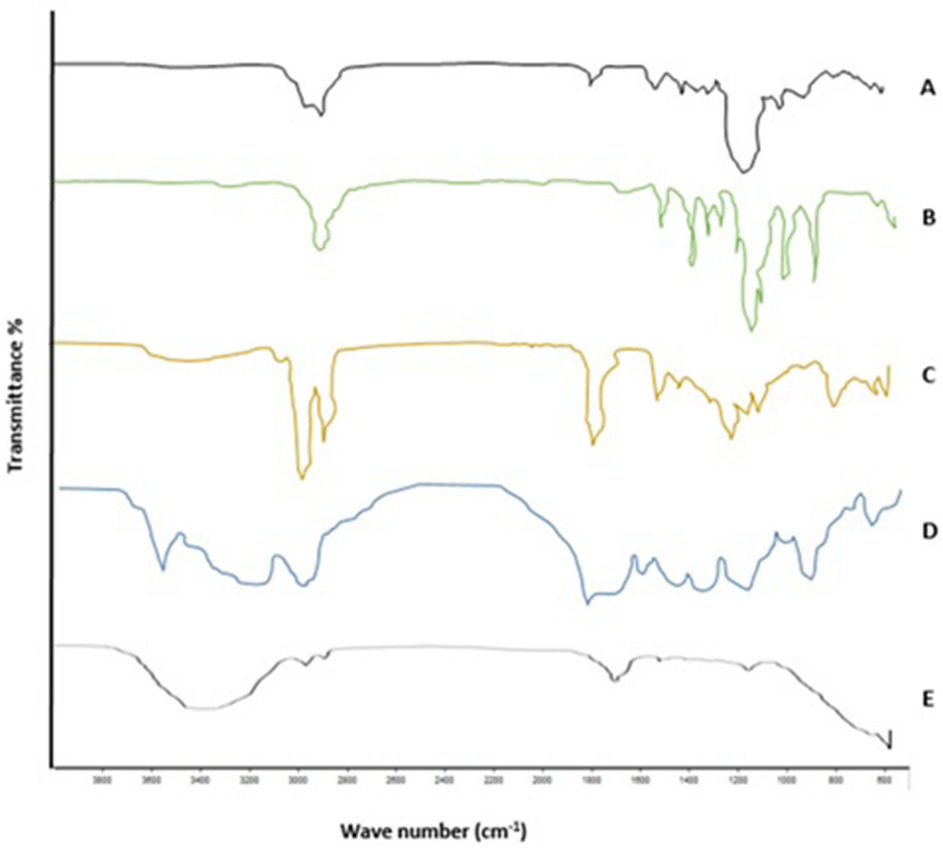


**Figure 6** FTIR spectral analysis. FTIR spectra of (**A**) Tween 80, (**B**) Poloxamer 188, (**C**) glyceryl monooleate, (**D**) pure CPB, and (**E**) CPB-loaded cubosomes, confirming functional group compatibility and absence of chemical interactions among formulation components.

## Stability Studies

### Centrifugation Stability

After centrifugation, no phase separation, creaming, or sedimentation was observed, indicating that the cubosomes have strong physical stability and resistance to shear stress. The absence of visible structural disruption confirms effective stabilization by Pluronic F-68 and glyceryl monooleate.

### Freeze–Thaw Stability

Freeze–thaw cycling did not cause aggregation, precipitation, or phase separation. The maintained clarity and uniformity after repeated cycles demonstrate excellent thermal stability, suggesting that the structural integrity of the cubic matrix remains intact even under extreme temperature fluctuations.

### Differential Scanning Calorimetry (DSC)

The DSC thermograms (Figure 7) provided important insights into the thermal behavior and physical state of CPB within the cubosomal formulation. Pure CPB showed a distinct, sharp endothermic peak at approximately 110°C, characteristic of its crystalline nature and corresponding to its melting point. The individual excipients – glyceryl monooleate and Pluronic F-68—displayed their own melting transitions at 32–38°C and 55–60°C, respectively, confirming their crystalline or semi-crystalline thermal characteristics. In contrast, the DSC profile of the CPB-loaded cubosomes showed a markedly altered thermal pattern. The sharp melting peak of CPB was absent or replaced by a broadened, less intense thermal transition, indicating that the drug no longer existed in its native crystalline form. This shift to a broadened and lower-intensity endotherm suggests that CPB transformed into an amorphous or molecularly dispersed state within the lipid matrix. Such a transition typically occurs when the drug becomes fully integrated into the nanostructured lipid domains of the cubosomes. This thermal behavior strongly supports the successful encapsulation of CPB and confirms

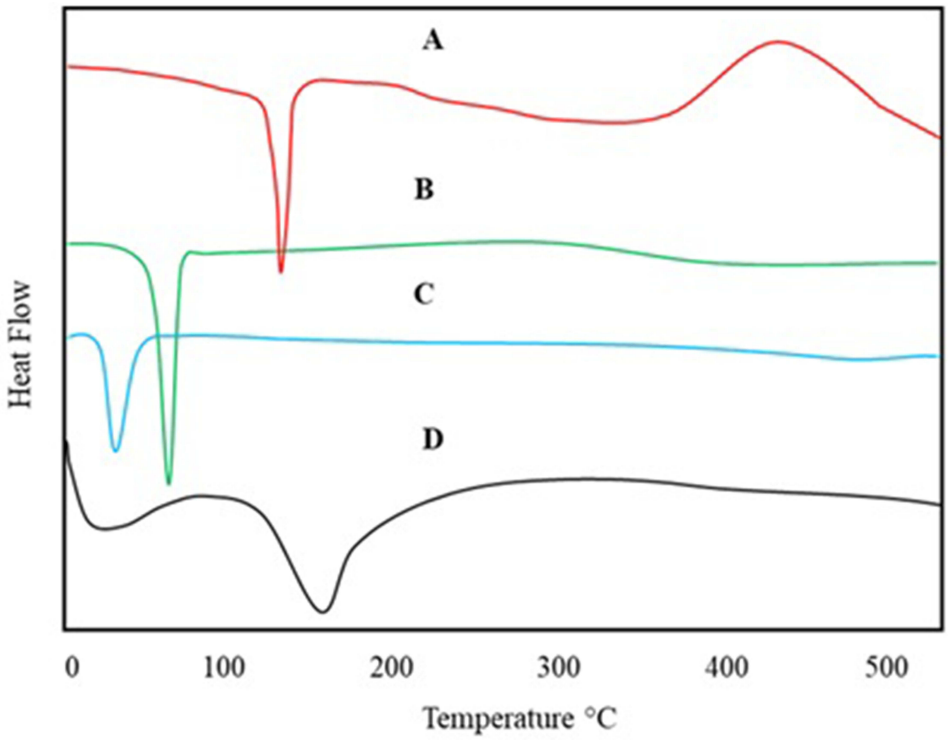


**Figure 7** Differential scanning calorimetry (DSC) thermograms. DSC thermograms of (**A**) CPB, (**B**) Poloxamer 188, (**C**) glyceryl monooleate, and (**D**) CPB-loaded cubosomal formulation, demonstrating changes in thermal behavior and reduced crystallinity of CPB upon cubosome incorporation.

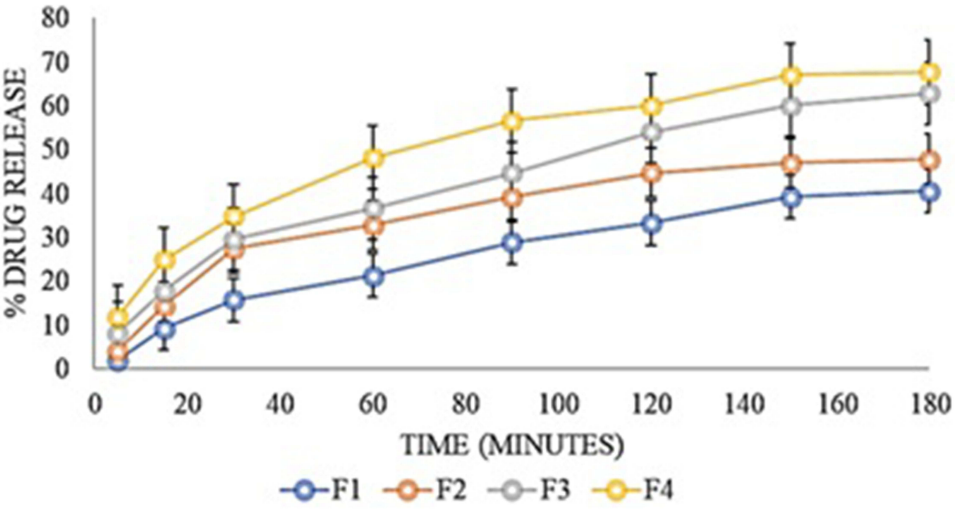


**Figure 8** In-vitro drug release profile of CPB-loaded cubosomes. Comparative in-vitro release profiles of CPB from cubosomal formulations, illustrating sustained and controlled drug release behavior over the study period.

that the drug is uniformly distributed within the lipid matrix, rather than remaining as a separate crystalline phase. Amorphization within the formulation is advantageous, as it can enhance drug solubility, improve dissolution rate, and contribute to more controlled and sustained release characteristics.

## In-vitro Drug Release and Permeation

The in-vitro drug release and permeation studies (Figures 8 and 9) collectively demonstrate the efficiency of the CPB-loaded cubosomal formulations in enabling both sustained drug release and enhanced transmembrane transport. All


https://doi.org/10.2147/DDDT.S574417

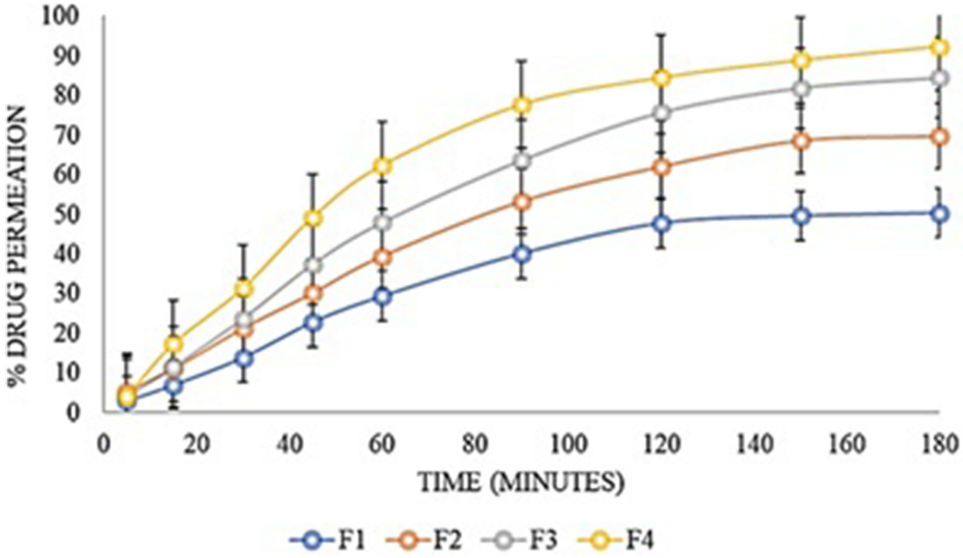


**Figure 9** In-vitro permeation studies of CPB-loaded cubosomes. In-vitro permeation profiles of CPB-loaded cubosomal formulations across a synthetic membrane, demonstrating enhanced transmembrane permeation compared with the control.

formulations showed a gradual, time-dependent increase in CPB release over 180 minutes, confirming the cubosomal matrix's ability to provide controlled diffusion through its bicontinuous lipid channels. Among the four formulations, F4 displayed the highest cumulative drug release, attributable to its higher levels of glyceryl monooleate and Pluronic F-68, which improved solubilization, increased matrix fluidity, and created more efficient diffusion pathways. A similar trend appeared in the permeation profiles, with all formulations showing progressive increases in CPB permeation across the synthetic membrane throughout the study period. F4 again achieved the greatest extent of permeation, approaching near-complete transport by 180 minutes and significantly outperforming F1, F2, and F3. This enhanced permeation efficiency reflects the synergistic effects of glyceryl monooleate – providing bioadhesion, membrane interaction, and structural flexibility – and Pluronic F-68, which improves wettability and reduces interfacial resistance. The consistent, stepwise increase in release and permeation across formulations corresponds with the strengthening cubic-phase nanostructure as the concentrations of lipid and surfactant increase. Together, the release and permeation results underscore the strong capability of cubosomes to modulate drug transport through both controlled release from the nanostructure and effective permeation across biological barriers. These findings highlight the formulation's potential to maintain sustained drug availability, improve therapeutic uptake, and serve as a promising platform for topical and transdermal delivery of CPB and other poorly soluble drugs.

## Discussion

This study successfully developed and characterized capecitabine (CPB)-loaded cubosomal formulations, demonstrating their suitability as an effective dermal and transdermal drug delivery platform. Each evaluated physicochemical parameter provides insight into the performance, stability, and therapeutic potential of the cubosomes. The pH of the formulations (5.9–6.4) is within the physiologically acceptable range for dermal application, ensuring minimal irritation and favorable patient compliance. Skin-compatible formulations generally maintain a pH between 4.5 and 6.5 to preserve barrier function and prevent inflammatory responses, consistent with previous observations in topical nanocarrier systems.[62,63] The cubosomes show low viscosity which enables better spreadability and improved patient comfort and fast drug penetration through the application area. Research indicates that lower-viscosity systems improve drug distribution within the skin while simultaneously speeding up the process of stratum corneum penetration.[64] The properties indicate that the cubosomal matrix serves as a stable system which works well for skin applications. The optimized formulation contains nanoparticles which measure approximately 177 nanometers in size at the nanoscale. The skin permeability of nanocarriers less than 200 nm improves because their small size creates more surface area which

enables better contact with skin lipid structures.[65,66] The SEM images showed that the cubic-shaped particles existed as separate well-distributed cubic particles which proved that the cubosomal nanostructure remained intact. The particle size decreases as Pluronic F-68 concentrations rise because F4 shows the most significant effect due to its steric stabilization properties. The self-assembly process benefits from poloxamers because they decrease surface tension and stop particle merging and enable the creation of homogeneous nanostructures.[67] This finding aligns with earlier reports demonstrating the role of Pluronic surfactants in stabilizing bicontinuous cubic phases in lipid-based drug delivery systems.[68,69]

The transformation of CPB from a crystalline to an amorphous state in the cubosomal formulation, indicated by the disappearance of characteristic drug peaks in the XRD pattern, strongly suggests successful encapsulation. Amorphization is desirable because it enhances solubility and dissolution kinetics, thereby improving overall bioavailability.[8,9] FTIR analysis further confirmed the absence of significant chemical shifts or degradation peaks, indicating compatibility between CPB and the excipients. The retention of characteristic functional groups shows that the drug was incorporated physically without chemical modification. Similar results have been reported in other cubosomal drug delivery studies, where excipient drug compatibility was crucial for maintaining formulation stability.[10,11]

DSC thermograms supported the XRD findings, as the sharp endothermic peak of pure CPB disappeared and was replaced by a broad, diffuse peak in the formulation. This change indicates molecular dispersion of CPB within the lipid matrix and supports the hypothesis of amorphization.[12] Molecularly dispersed drug states are associated with improved solubilization, reduced risk of recrystallization, and prolonged release patterns.[13] The endothermic transitions corresponding to glyceryl monooleate and Pluronic F-68 remained visible, confirming that the structural integrity of the excipients was retained during formulation. The cubosomal formulations showed excellent stability under centrifugation and freeze thaw conditions, with no phase separation or sedimentation observed. Physical stability is essential for nanocarriers, as destabilization can cause aggregation, altered release kinetics, and loss of therapeutic efficacy. Reports indicate that cubic-phase nanostructures inherently have high thermodynamic stability due to their bicontinuous lipid arrangement and steric stabilization by nonionic surfactants.[14] The ability of the cubosomes to withstand stress conditions demonstrates robustness in formulation and potential suitability for storage, transport, and long-term use.

The in vitro release and permeation data showed that formulation F4 had the highest drug release and transmembrane permeation. This improvement is attributed to its higher concentrations of Pluronic F-68 and glyceryl monooleate, which together increase membrane fluidization, solubilization capacity, and the diffusion rate of CPB.[15] Cubic-phase lipid systems are known for controlled and sustained release due to their tortuous internal channel networks that modulate diffusion.[16] Additionally, the amphiphilic nature of glyceryl monooleate disrupts lipid packing in the stratum corneum, creating transient pathways for improved drug transport.[17] These results are consistent with previous studies demonstrating enhanced dermal delivery of chemotherapeutics and hydrophilic drugs using cubosome-based carriers.[18,19] Overall, the results highlight that CPB-loaded cubosomes, particularly formulation F4, offer a promising strategy for topical and transdermal delivery. Their suitable pH, favorable viscosity, nanoscale size, amorphous drug encapsulation, high stability, and superior release and permeation profiles collectively support their potential for improved therapeutic performance.

## Conclusion

The findings of this study clearly demonstrate the strong potential of cubosome-based systems as an innovative platform for enhancing the delivery of therapeutic agents. The formulated CPB-loaded cubosomes exhibited the key attributes of an efficient nanocarrier: structural stability, favorable biocompatibility, and the ability to improve drug diffusivity and permeation across biological barriers. These results reinforce the growing recognition of cubosomes as versatile, next-generation lipid nanostructures capable of overcoming solubility limitations, enhancing drug penetration, and enabling more controlled and sustained delivery profiles. Their unique bicontinuous cubic phase offers a high internal surface area and tunable architecture, supporting their suitability for a wide range of pharmaceutical applications, particularly in dermal, transdermal, and targeted therapeutic interventions.

The potential of cubosome technology extends beyond the present findings, offering significant scope for future research and clinical application. Their inherent adaptability allows for functionalization with ligands, peptides, antibodies, and stimuli-responsive materials, creating opportunities for precision therapy and personalized drug delivery. Cubosomes also show promise for encapsulating diverse therapeutic agents, including peptides, nucleic acids, and

biologics, broadening their impact across multiple treatment domains. Further investigations into pharmacokinetics, long-term safety, in vivo performance, and manufacturability will be essential to advance their translation from laboratory innovation to clinical reality. Taken together, these perspectives highlight cubosomes as a transformative nanocarrier platform with substantial potential to enhance therapeutic efficacy, reduce systemic toxicity, and influence the next generation of advanced drug delivery technologies.

## Data Sharing Statement

The data and materials are available upon reasonable request from the corresponding author.

## Consent for Publication

The author has read and agreed to the published version of the manuscript.

## Acknowledgments

The author gratefully acknowledges the funding of the Deanship of Graduate Studies and Scientific Research, Jazan University, Saudi Arabia, through project number: (RG24-M015).

## Author Contributions

The author made a significant contribution to the work reported, whether that is in the conception, study design, execution, acquisition of data, analysis and interpretation, or in all these areas; took part in drafting, revising or critically reviewing the article; gave final approval of the version to be published; have agreed on the journal to which the article has been submitted; and agree to be accountable for all aspects of the work.

## Funding

The author gratefully acknowledges the funding of the Deanship of Graduate Studies and Scientific Research, Jazan University, Saudi Arabia, through project number: (RG24-M015).

## Disclosure

The author declares that there is no financial or other conflict of interest associated with this study.

## References

1. Siegel RL, Miller KD, Wagle NS, Jemal A. Cancer statistics, 2022. *CA*. 2022;72(1):7–33.
2. Howlader N, Forjaz G, Mooradian MJ, et al. The effect of advances in lung-cancer treatment on population mortality. *New Engl J Med*. 2020;383 (7):640–649. doi:10.1056/NEJMoa1916623
3. Yekedüz E, Utkan G, Ürün Y. A systematic review and meta-analysis: the effect of active cancer treatment on severity of COVID-19. *Eur J Cancer*. 2020;141:92–104. doi:10.1016/j.ejca.2020.09.028
4. Souza e Silva V, Chinen LTD, Abdallah EA, et al. Early detection of poor outcome in patients with metastatic colorectal cancer: tumor kinetics evaluated by circulating tumor cells. *OncoTargets Ther*. 2016;9:7503–7513. doi:10.2147/OTT.S115268
5. Hossain MS, Karuniawati H, Jairoun AA, et al. Colorectal cancer: a review of carcinogenesis, global epidemiology, current challenges, risk factors, preventive and treatment strategies. *Cancers*. 2022;14(7):1732. doi:10.3390/cancers14071732
6. Tolba MF. Revolutionizing the landscape of colorectal cancer treatment: the potential role of immune checkpoint inhibitors. *Int J Cancer*. 2020;147 (11):2996–3006. doi:10.1002/ijc.33056
7. Han CJ, Yang GS, Syrjala K. Symptom experiences in colorectal cancer survivors after cancer treatments: a systematic review and meta-analysis. *Cancer Nurs*. 2020;43(3):E132–E158. doi:10.1097/NCC.0000000000000785
8. Henry JT, Johnson BJCCO. Current and evolving biomarkers for precision oncology in the management of metastatic colorectal cancer. *Chin Clin Oncol*. 2019;8(5):49.
9. Caiado J, Brás R, Paulino M, et al. Rapid desensitization to antineoplastic drugs in an outpatient immunoallergology clinic: outcomes and risk factors. *Annals Allergy Asthma Immunol*. 2020;125(3):325–333.e1. doi:10.1016/j.anai.2020.04.017
10. Duarte D, Vale N. New trends for antimalarial drugs: synergism between antineoplastics and antimalarials on breast cancer cells. *Biomolecules*. 2020;10(12):1623. doi:10.3390/biom10121623
11. Ishikawa T, Utoh M, Sawada N, et al. Tumor selective delivery of 5-fluorouracil by capecitabine, a new oral fluoropyrimidine carbamate, in human cancer xenografts. *Biochem Pharmacol*. 1998;55(7):1091–1097. doi:10.1016/s0006-2952(97)00682-5
12. Davis DW, Herbst RS, Abbruzzese JL, Eds.. *Antiangiogenic Cancer Therapy*. 1st ed. CRC Press; 2007. doi:10.1201/9781420004298
13. Cao Y, Alamri S, Rajhi AA, Anqi AE, Derakhshandeh M. The capability of boron carbide nanotube as a nanocarrier for fluorouracil anticancer drug delivery; DFT study. *Mat Chem Phys*. 2022;275:125260.

14. Vale N, Pereira M, Santos J, et al. Prediction of drug synergism between peptides and antineoplastic drugs Paclitaxel, 5-Fluorouracil, and Doxorubicin using in silico approaches. *Int J Mol Sci*. 2022;24(1):69. doi:10.3390/ijms24010069
15. Schüller J, Cassidy J, Dumont E, et al. Preferential activation of capecitabine in tumor following oral administration to colorectal cancer patients. *Cancer Chemother Pharmacol*. 2000;45:291–297. doi:10.1007/s002800050043
16. Ayyanaar S, Bhaskar R, Esthar S, et al. Design and development of 5-fluorouracil loaded biodegradable magnetic microspheres as site-specific drug delivery vehicle for cancer therapy. *J Magnet Magnetic Mat*. 2022;546:168853. doi:10.1016/j.jmmm.2021.168853
17. Asif M, Sajid H, Ayub K, et al. Therapeutic potential of oxo-triarylmethyl (oxTAM) as a targeted drug delivery system for nitrosourea and fluorouracil anticancer drugs; A first principles insight. *J Mol Graphics Model*. 2023;122:108469. doi:10.1016/j.jmgm.2023.108469
18. Lee W, Song G, Bae H. Matairesinol induces mitochondrial dysfunction and exerts synergistic anticancer effects with 5-fluorouracil in pancreatic cancer cells. *Marine Drugs*. 2022;20(8):473. doi:10.3390/md20080473
19. Wainberg ZA, Feeney K, Lee MA, et al. Meta-analysis examining overall survival in patients with pancreatic cancer treated with second-line 5-fluorouracil and oxaliplatin-based therapy after failing first-line gemcitabine-containing therapy: effect of performance status and comparison with other regimens. *BMC Cancer*. 2020;20:1–9.
20. Rehman U, Sarfraz RM, Mahmood A, et al. pH Responsive Hydrogels for the Delivery of Capecitabine: development, Optimization and Pharmacokinetic Studies. *Gels*. 2022;8(12):775. doi:10.3390/gels8120775
21. Otsu T, Inokawa Y, Takami H, et al. Comparison between FOLFIRINOX and nal-IRI/FL as second-line treatment after gemcitabine plus nab-paclitaxel for pancreatic cancer. *Anticancer Res*. 2022;42(8):3889–3894. doi:10.21873/anticanres.15882
22. De Dosso S, Siebenhüner AR, Winder T, et al. Treatment landscape of metastatic pancreatic cancer. *Cancer Treatment Rev*. 2021;96:102180. doi:10.1016/j.ctrv.2021.102180
23. Pal N, Li H, You S, et al. Phase behaviour and characterization of microemulsion stabilized by a novel synthesized surfactant: implications for enhanced oil recovery. *Chemosphere*. 2019;235:995–1009. doi:10.1016/j.chemosphere.2019.07.025
24. Gagliardi A, Cosco D, Udongo BP, et al. Design and characterization of glyceryl monooleate-nanostructures containing doxorubicin hydrochloride. *Pharmaceutics*. 2020;12(11):1017. doi:10.3390/pharmaceutics12111017
25. Elsayed A, Belal A, Al-Sou'od K. Preparation and optimization of glyceryl monooleate-low molecular weight chitosan nanoparticles for delivery of morpholinopyrrolizine derivative. *Trop J Pharmaceut Res*. 2022;21(9):1813–1821. doi:10.4314/tjpr.v21i9.1
26. Moshikur RM, Ali MK, Moniruzzaman M, Goto M. Recent advances in surface-active ionic liquid-assisted self-assembly systems for drug delivery. *Current Opinion Colloid Interface Sci*. 2021;56:101515.
27. Atlıbatur R, Bahadori F, Kizilcay GE, et al. Preparation and characterization of glyceryl dibehenate and glyceryl monostearate-based lyotropic liquid crystal nanoparticles as carriers for hydrophobic drugs. *J Drug Delivery Sci Technol*. 2023;87:104821. doi:10.1016/j.jddst.2023.104821
28. Patil P, Killedar S. Chitosan and glyceryl monooleate nanostructures containing gallic acid isolated from amla fruit: targeted delivery system. *Heliyon*. 2021;7(3):e06526. doi:10.1016/j.heliyon.2021.e06526
29. Davis DA, Martins PP, Zamloot MS, et al. Complex drug delivery systems: controlling transdermal permeation rates with multiple active pharmaceutical ingredients. *AAPS PharmSciTech*. 2020;21:1–11.
30. Shiadeh SNR, Khodaverdi E, Maleki MF, et al. A sustain-release lipid-liquid crystal containing risperidone based on glycerol monooleate, glycerol dioleate, and glycerol trioleate: in-vitro evaluation and pharmacokinetics in rabbits. *J Drug Delivery Sci Technol*. 2022;70:103257. doi:10.1016/j.jddst.2022.103257
31. Gowda BJ, Ahmed MG, Alshehri SA, et al. The cubosome-based nanoplatforms in cancer therapy: seeking new paradigms for cancer theranostics. *Environ Res*. 2023;237:116894. doi:10.1016/j.envres.2023.116894
32. Said S, Mikhail S, Riad MJMSFET. Recent processes for the production of alumina nano-particles. *Commun Biol*. 2020;3:344–363. doi:10.1038/s42003-020-1071-5
33. Alharbi WS, Hosny KM. Development and optimization of ocular in situ gels loaded with ciprofloxacin cubic liquid crystalline nanoparticles. *J Drug Delivery Sci Technol*. 2020;57:101710. doi:10.1016/j.jddst.2020.101710
34. Dully M, Brasnett C, Djeghader A, et al. Modulating the release of pharmaceuticals from lipid cubic phases using a lipase inhibitor. *J Colloid Interface Sci*. 2020;573:176–192. doi:10.1016/j.jcis.2020.04.015
35. Kaur SD, Singh G, Singh G, et al. Cubosomes as potential nanocarrier for drug delivery: a comprehensive review. *J Pharmaceut Res Int*. 2021;33(31B):118–135. doi:10.9734/jpri/2021/v33i31B31698
36. Dhadwal A, Raj SD, Vinay P, Singh AM, Pravin K. Cubosomes: a novel carrier for transdermal drug delivery. 2020;10(1):123–130.
37. Bala R, Sindhu RK, Kaundle B, et al. The prospective of liquid crystals in nano formulations for drug delivery systems. *J Mol Struct*. 2021;1245:131117. doi:10.1016/j.molstruc.2021.131117
38. Abourehab MA, Ansari MJ, Singh A, et al. Cubosomes as an emerging platform for drug delivery: a review of the state of the art. *J Mat Chem B*. 2022;10(15):2781–2819. doi:10.1039/D2TB00031H
39. Sepulveda AF, Kumpgdee-Vollrath M, Franco MKKD, et al. Supramolecular structure organization and rheological properties modulate the performance of hyaluronic acid-loaded thermosensitive hydrogels as drug-delivery systems. *J Colloid Interface Sci*. 2023;630:328–340. doi:10.1016/j.jcis.2022.10.064
40. Naidjonoka P, Fornasier M, Pålsson D, et al. Bicontinuous cubic liquid crystalline phase nanoparticles stabilized by softwood hemicellulose. *Colloids Surfaces B Biointerfaces*. 2021;203:111753. doi:10.1016/j.colsurfb.2021.111753
41. Nasr M, Almawash S, Al Saqr A, et al. Bioavailability and antidiabetic activity of gliclazide-loaded cubosomal nanoparticles. *Pharmaceuticals*. 2021;14(8):786. doi:10.3390/ph14080786
42. Alamoudi J, Almoshari Y, Alotaibi H. Fabrication and evaluation of poloxamer facilitated, glyceryl monooleate based 5-fluorouracil cubosomes. *Ind J Pharmaceut Educ Res*. 2023;58:91–98. doi:10.5530/ijper.58.1.9
43. Fornasier M, Pireddu R, Del Giudice A, et al. Tuning lipid structure by bile salts: hexosomes for topical administration of catechin. *Colloids Surfaces B Biointerfaces*. 2021;199:111564.
44. Chettupalli AK, Ananthula M, Amarachinta PR, Bakshi V, Yata VK. Design, formulation, in-vitro and ex-vivo evaluation of atazanavir loaded cubosomal gel. *Biointerface Res Appl Chem*. 2021;11(4):12037–12054.
45. Sarkar S, Tran N, Soni SK, et al. Size-dependent encapsulation and release of dsDNA from cationic lyotropic liquid crystalline cubic phases. *ACS Biomat Sci Eng*. 2020;6(8):4401–4413. doi:10.1021/acsbiomaterials.0c00085

46. Alamoudi J, Almoshari Y, Alotaibi H. Formulation and evaluation of pluronic F-127 assisted carboplatin cubosomes. *Ind J Pharmaceut Educ Res*. 2023;57:1258–1264. doi:10.5530/ijper.57.4.150
47. Sarker M, Yeasmin M, Al-Mamun MA, et al. Influence of Gd content on the structural, Raman spectroscopic and magnetic properties of CoFe2O4 nanoparticles synthesized by sol-gel route. *Ceramics Int*. 2022;48(22):33323–33331. doi:10.1016/j.ceramint.2022.07.275
48. Singhal K, Kaushik N, Kumar AJCDD. Cubosomes: versatile nanosized formulation for efficient delivery of therapeutics. *Current Drug Delivery*. 2022;19(6):644–657. doi:10.2174/1567201818666210708123855
49. Lai X, Ding Y, Wu C-M, et al. Phytantriol-based cubosome formulation as an antimicrobial against lipopolysaccharide-deficient gram-negative bacteria. *ACS Appl Mat Interfaces*. 2020;12(40):44485–44498. doi:10.1021/acsami.0c13309
50. Palan F, Pai R, Chatterjee B, et al. Cubosomes–A novel approach to taste masking using ibuprofen as a model drug. *J Dispersion Sci Technol*;2024. 1–11. doi:10.1080/01932691.2024.2417691
51. Zakaria F, Ashari SE, Azmi ID, Rahman MB. Recent advances in encapsulation of drug delivery (active substance) in cubosomes for skin diseases. *J Drug Deliv Sci Technol*. 2022;103097.
52. Kaul S, Nagaich U, Verma N. Preclinical assessment of nanostructured liquid crystalline particles for the management of bacterial keratitis: in vivo and pharmacokinetics study. *Drug Delivery Transl Res*. 2022;12:1–19.
53. Deruyver L, Rigaut C, Gomez-Perez A, et al. In vitro evaluation of paliperidone palmitate loaded cubosomes effective for nasal-to-brain delivery. *Int J Nanomed*. 2023;Volume 18:1085–1106. doi:10.2147/IJN.S397650
54. Nasr M, Ghorab MK, Abdelazem AJAPSB. In vitro and in vivo evaluation of cubosomes containing 5-fluorouracil for liver targeting. *Acta pharmaceutica sinica B*. 2015;5(1):79–88. doi:10.1016/j.apsb.2014.12.001
55. Akhlaghi SP, Ribeiro IR, Boyd BJ, et al. Impact of preparation method and variables on the internal structure, morphology, and presence of liposomes in phytantriol-Pluronic® F127 cubosomes. *Colloids Surfaces B Biointerfaces*. 2016;145:845–853. doi:10.1016/j.colsurfb.2016.05.091
56. Bei D, Marszalek J, Youan B-BC. Formulation of dacarbazine-loaded cubosomes—part I: influence of formulation variables. *Aaps PharmScitech*. 2009;10(3):1032–1039. doi:10.1208/s12249-009-9293-3
57. Farooq M, Usman F, Naseem M, et al. Voriconazole cyclodextrin based polymeric nanobeads for enhanced solubility and activity: in vitro/in vivo and molecular simulation approach. *Pharmaceutics*. 2023;15(2):389. doi:10.3390/pharmaceutics15020389
58. Shafiq S, Shakeel F, Talegaonkar S, et al. Development and bioavailability assessment of ramipril nanoemulsion formulation. *Eur J Pharmaceut Biopharmaceut*. 2007;66(2):227–243. doi:10.1016/j.ejpb.2006.10.014
59. Yap SL, Yu H, Li S, et al. Cell interactions with lipid nanoparticles possessing different internal nanostructures: liposomes, bicontinuous cubosomes, hexosomes, and discontinuous micellar cubosomes. *J Colloid Interface Sci*. 2024;656:409–423. doi:10.1016/j.jcis.2023.11.059
60. Hosny KM. Nanosized cubosomal thermogelling dispersion loaded with saquinavir mesylate to improve its bioavailability: preparation, optimization, in vitro and in vivo evaluation. *Int J Nanomed*. 2020;Volume 15:5113–5129. doi:10.2147/IJN.S261855
61. Nandgude TD, Bhise KS, Gupta VB, et al. Characterization of hydrochloride and tannate salts of diphenhydramine. *Ind J Pharmaceut Sci*. 2008;70 (4):482–486. doi:10.4103/0250-474X.44598
62. Bouwstra JA. Structure of the skin barrier and its modulation by vesicular formulations. *Progress Lipid Res*. 2003;42(1):1–36. doi:10.1016/S0163-7827(02)00028-0
63. Lodén M, Buraczewska I, Edlund F. The irritation potential and reservoir effect of mild soaps. *Contact Dermat*. 2003;49(2):91–96. doi:10.1111/j.0105-1873.2003.00186.x
64. Sivadasan D, Sultan MH, Alqahtani SS, Javed S. Cubosomes in drug delivery—A comprehensive review on its structural components, preparation techniques and therapeutic applications. *Biomedicines*. 2023;11(4):1114. doi:10.3390/biomedicines11041114
65. Attri N, Das S, Banerjee J, Shamsuddin SH, Dash SK, Pramanik A. Liposomes to cubosomes: the evolution of lipidic nanocarriers and their cutting-edge biomedical applications. *ACS Appl Bio Mat*. 2024;7(5):2677–2694. doi:10.1021/acsabm.4c00153
66. Nath AG, Dubey P, Kumar A, et al. Recent advances in the use of cubosomes as drug carriers with special emphasis on topical applications. *J Lipids*. 2024;2024(1):Article2683466. doi:10.1155/2024/2683466
67. Matloub AA, AbouSamra MM, Salama AH, Rizk MZ, Aly HF, Fouad GI. Cubic liquid crystalline nanoparticles containing a polysaccharide from Ulva fasciata with potent antihyperlipidaemic activity. *Saudi Pharmaceut J*. 2018;26(2):224–231. doi:10.1016/j.jsps.2017.12.007
68. Chong JYT, Mulet X, Boyd BJ, Drummond CJ. Steric stabilizers for cubic phase lyotropic liquid crystal nanodispersions (cubosomes). In: *Advances in Planar Lipid Bilayers and Liposomes*. Vol. 21. Academic Press;2015:131–187. doi:10.1016/bs.adplan.2014.11.001
69. Khan S, Madni A, Rahim MA, et al. Enhanced in vitro release and permeability of glibenclamide by proliposomes: development, characterization and histopathological evaluation. *J Drug Deliv Sci Technol*. 2021;63:102450.